Measuring the Strain-Temperature Phase Diagram of Vanadium Dioxide Nanowires

Eli Bingham*
University of North Carolina at Chapel Hill

Vanadium dioxide (VO_2) is a strongly correlated material that undergoes an abrupt first-order phase transition at about 68°C in bulk crystals from an insulating state to a metallic state, changing the conductivity by more than four orders of magnitude. We apply strain and heat to VO_2 nanowires to study the phase diagram of undoped and Al-doped VO_2. We also report the first optical measurements of the M1-M2 phase boundary and a novel measurement technique for relative lattice constants of all three optically-distinguishable phases.

I. INTRODUCTION

Vanadium dioxide (VO_2) is a strongly correlated material that undergoes an abrupt first-order phase transition at about $T_c \approx 68°C$ in bulk crystals from an insulating state to a metallic state, changing the conductivity by more than four orders of magnitude. The remarkable properties of this transition are interesting for both applied and fundamental reasons; for more than 50 years there has been active experimental and theoretical work on the use of VO_2 as the material for a Mott transistor, a hypothetical device based on metal-insulator transitions. In optical pump-probe measurements the transition appears to be intrinsically ultrafast, occurring in as little as 100 femtoseconds in thin films[5]. The metal state is also much less optically transparent than the insulating state[6], suggesting possible applications in ultrafast optical shutters. Finally, in most metals, we can treat the charge carriers theoretically as a Fermi liquid. However, Fermi liquid theory breaks down when interactions between electrons become too strong, so the mechanism and fundamental properties of the metal-insulator transition in VO_2 are still poorly understood theoretically[1]. VO_2 is therefore interesting as a model strongly correlated system with properties that can be extrapolated to other, more complicated systems.

VO_2 exhibits four phases in our region of interest, though there is some debate as to whether one is a mixture of two of the others rather than a distinct phase. Above T_c, free crystals become metallic and the vanadium atoms form periodic chains along the c-axis, so this phase is known as the rutile phase. Below T_c, free VO_2 crystals are in a monoclinic insulating phase called M1 where the vanadium atoms form distorted dimers along the rutile c-axis. If the crystals are doped or placed under tension, they can undergo a first-order transition to a different insulating phase called M2 where the vanadium atoms are not all dimerized. The fourth phase is known in the literature as the triclinic phase and stabilizes under compression and lower temperatures[2]. We are mainly interested in M1, M2, and R, since there is no T-R transition and T-M1 and T-M2 transitions are second-order and therefore not observable optically.

Nanowires of VO_2 are an ideal place to study these phase transitions because they are smaller than the characteristic domain structure of VO_2, allowing clean nucleations of and fine control over single metallic or insulating domains that can be repeatedly, reproducibly manipulated without damaging the sample[2]. The reason this setup allows such precise control over the interphase boundaries follows from the differences in the length of the c-axis in unit cells of each phase. If a nanowire is cantilevered or otherwise free to change its length, it will undergo a sudden, whole-wire phase transition at the appropriate temperature. However, if the length is fixed somehow (e.g. by suspending a wire across a gap and gluing down the ends), the phase transition is not energetically favourable throughout the whole wire because the usual change in length would place it under high tensile or compressive strain. Instead, the wire goes into coexistence and creates an interphase boundary. Precise control of the natural wire length therefore allows continuous creation of either the shorter or longer phase[2].

My project this summer was to make strain devices, help design the next version of the strain system, and do measurements with the ultimate goal of precisely mapping the strain-temperature phase diagram of VO_2. I also worked on a potential way to make strain-free devices and tunneling devices using graphene electrical contacts, implemented a nanostructure transfer technique[3] and graphene production system[4], and helped make some samples for ultrafast measurements of the metal-insulator transition of VO_2 crystals on top of graphite and boron nitride on diamond and sapphire substrates, but all of those are beyond the scope of this paper.

II. DEVICE FABRICATION

A. Wire synthesis

VO_2 nanowires were grown by physical vapor deposition (PVD) using the following procedure: A small amount of V_2O_5 powder was placed on a crucible, which was then placed in a glass tube about 2cm away from the target chip. The tube was placed in a growth oven and evacuated, then refilled with argon. The oven was heated to $950°C$ while argon flowed continuously, so that evaporated V_2O_5 moved downstream from the crucible to the target and condensed on the target as VO_2 (depending on the amount of source and the distance between source and target, different kinds of VO_2 crystals can be syn-

Figure 1: The oven and compressed argon used for PVD of VO_2

thesized, e.g. plates, films, or wires). A catalyst (affectionately called "Steroids", actually AZ1500-series photoresist developer) can be deposited on the target chip to substantially increase the wire yield and average size.

Aluminum-doped nanowires were grown using a similar procedure as above, but a thin film of aluminum was evaporated onto the target chip before wire growth. To confirm that the wires had stabilized M2 at T_{room}, Raman spectroscopy (the standard method in the literature for determining the phase of VO_2) was performed on randomly selected Al-doped wires until appropriate samples could be selected for transfer.

B. Chip preparation

The chips are Si-SiO_2 wafers with "paddles" that can be pushed on to shrink the gap between the paddle and the rest of the chip, applying strain to anything suspended across the gap. The paddles were created using deep reactive-ion etching (DRIE), a technology that allows the creation of deep, narrow features like trenches and holes in silicon wafers. Gold electrical contacts were placed on the chip using photolithography or shadow evaporation before etching (the gap went through those as well), and after VO_2 was transferred across the gap the contacts were wirebonded to larger gold pads further up the chip.

C. Wire transfer, electrical contacts, and adhesion

We used a nanomanipulator to pick up individual nanowires from the growth chip and place them across the gaps in the paddles. The wires tend to bond to the SiO_2, but they can be scratched with the needle and lifted off the substrate by the van der Waals forces from the needle tip. The wires are then placed across the gap onto the SiO_2 (not the gold, because the wires will not come off the needle onto the gold) by contact between the wire and the substrate.

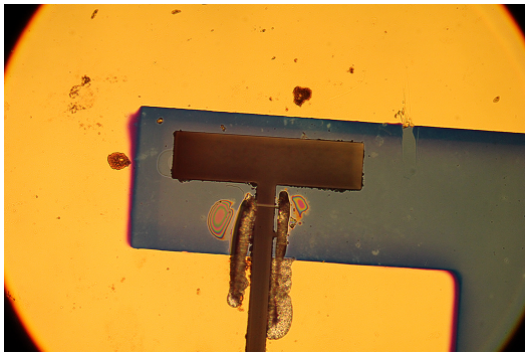

Figure 2: A complete device

After the wire is aligned as close to perpendicular to the gap as possible (to ensure that the strain is uniaxial and to prevent formation of multiple domains), the paddle chip is heated on a temperature stage alongside a small amount of indium. At a sufficiently high temperature, the manipulator and a different needle are used to pick up molten indium and put it down in a line from the wire to the nearby gold contact on each side of the gap. Unfortunately, in many later devices we were unable to make transport measurements due to a batch of chips with bad gold contacts, so the indium step was skipped in those.

Finally, we let the device cool down to room temperature and use the manipulator to apply ultraviolet-curable epoxy to each end of the wire. Capillary force draws the epoxy along the wire until it reaches the gap, where it stops because its viscosity is too high to run across or into the gap. The epoxy is cured in a UV light source for 15 minutes until it hardens and the wire is firmly attached to the substrate. Heat-activated epoxy must also be heated at 125°C for 10 minutes after UV exposure.

III. EXPERIMENT

A. Setup

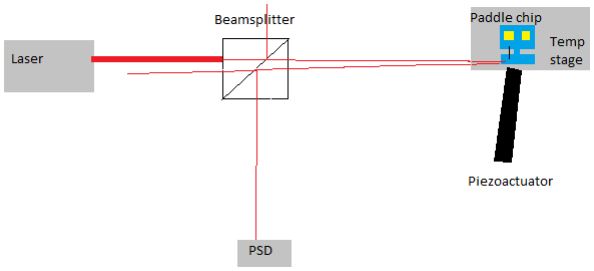

Figure 3: Strain setup schematic. Between the beamsplitter and the chip there is a quartz tube that the laser travels through to eliminate noise from turbulent flow in the air around the temperature stage.

The system used to apply strain to nanocrystals (designed and built by David Cobden, Jae Park, and Jim Coy) is simple to understand. The paddle chip on which the nanowires are suspended is mounted in a slot on a temperature stage which is made from Invar and controlled with a Lake Shore 325 temperature controller. A piezo-actuator pushes on one side of the paddle, allowing for the application of tensile or compressive stress (both are necessary since M1 stabilizes under compression and M2 stabilizes under tension) to wires depending on the side of the paddle that the pusher is contacting. The deflection angle of the paddle is precisely measured by using a PSD to measure the position of a laser spot reflected from the paddle into a beamsplitter. Electrical transport properties were measured by fixing a PCB to the temperature stage with two protruding wires that contacted the large gold pads on the paddle chip. The whole system is mounted under a high-quality optical microscope with a Canon DSLR camera and all parameters and incoming data, including laser lock-in configuration, are viewed and manipulated within a single LabVIEW program.

B. Measurements

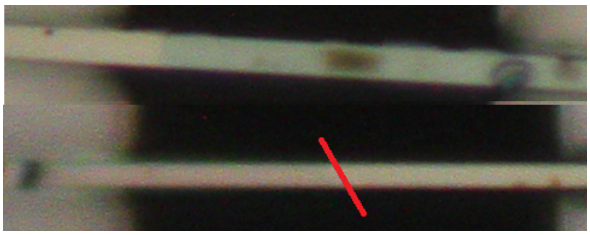

Figure 4: Top: an insulator-metal interphase boundary. Bottom: a M2-M1 interphase boundary emphasized with a red mark. The faint M1-M2 boundary is more noticeable while it is moving.

We took advantage of the wide coexistence regions in our devices to make several kinds of measurements, including preliminary optical measurements of the M1-M2 phase boundary which is visible only through a polarizer. The most basic was laser position versus interphase boundary position, i.e. applying progressively higher strain and recording the laser and boundary positions. Since this is essentially a measurement of rate of interconversion, the ratios of the slopes $\frac{dx}{dL}$ of the lines obtained from this data are actually the relative lattice constants between the various phases. Direct measurements of the edges of the coexistence regions in the phase diagram were made by making isobaric or isothermal sweeps and noting the nucleation temperature or strain of the new phase. Finally, changing the temperature and strain to keep the boundary position at a constant location in the gap allowed us to measure the middle of the coexistence regions. Later on we avoided taking data while decreasing the temperature, since VO_2 can undergo supercooling (visible in the constant x data presented in Figure 5 below).

Some devices also had electrical transport measurements to accompany the above, but many later devices did not. However, the lack of indium contacts made room for multiple wires on one hinge, greatly simplifying comparisons between wires.

IV. DATA AND RESULTS

A. Intrinsic VO_2

Our data (Figure 5) suggests qualitatively that the triple point of VO_2 is slightly below the transition temperature and just above the zero strain axis (in agreement with the literature), but unfortunately due to the nature of our setup probing the area just above and below zero strain is very difficult and we have therefore been unable to completely map out the phase diagram and precisely locate the triple point. We also made measurements like the ones in Figure 5 for every phase boundary, and while our relative lattice constants (see Measurements) are qualitatively correct (i.e. they are ordered correctly and fall around the known values), without the improvements to our setup described in Improvements and Future Work they are not consistent enough for us to make any stronger claims.

B. Aluminum-doped VO_2

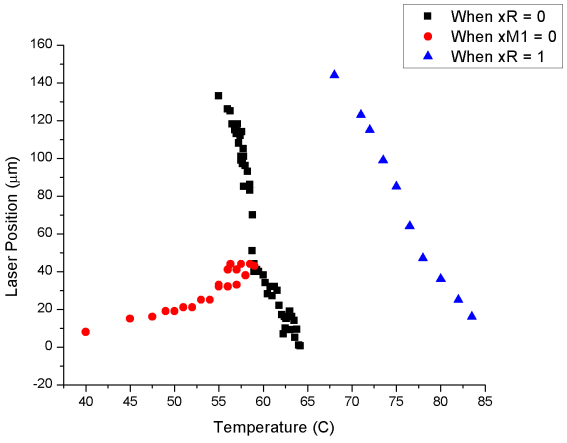

Figure 6: Strain-temperature phase diagram of Al-doped VO_2

Since aluminum doping stabilizes M2 in free crystals at T_{room} (confirmed with Raman spectroscopy) and seems to shift the entire phase diagram upwards in compressive stress, we are able to present preliminary measurements of the strain-temperature phase diagram of a $V_xAl_{1-x}O_2$

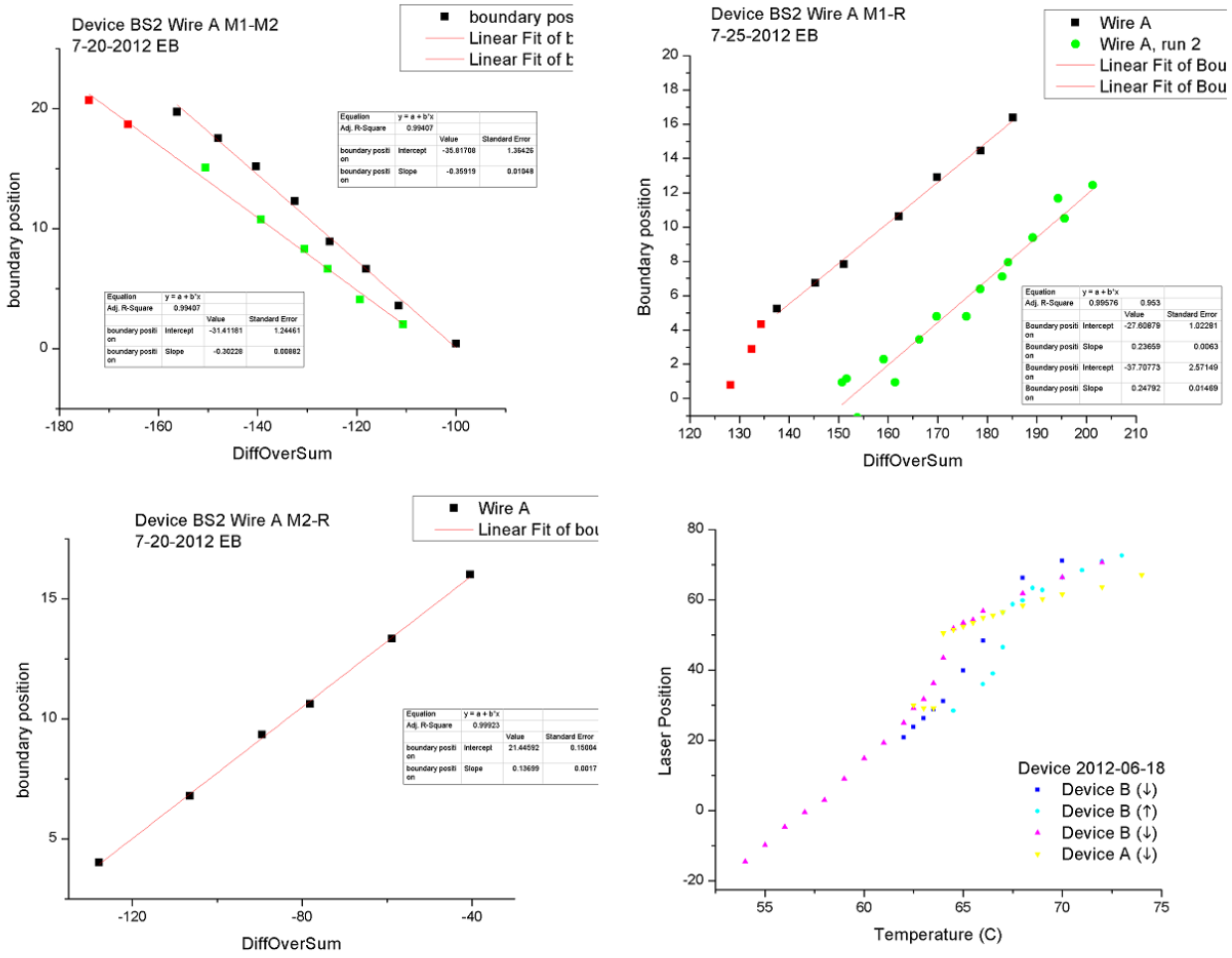

Figure 5: Examples of boundary position vs laser position and constant boundary position data in undoped VO_2. Strain is directly proportional to DiffOverSum (laser position). Clockwise from upper left: M1-M2 boundary vs. laser position; M1-R boundary vs. laser position; Constant x in an early device; M2-R boundary vs. laser position. Notice the abrupt change in slope in the constant x data just below the bulk T_c, especially in the cyan points which were taken while increasing temperature.

device with x not yet determined (X-ray diffraction measurements are planned for this device in the near future to precisely quantify the doping level). The red and black data in Figure 6 was obtained from isothermally compressing the wire until the uppermost phase nucleated; the blue points are where the wire became metallic across the entire gap region.

V. IMPROVEMENTS AND FUTURE WORK

There are many improvements that must be made to the strain setup and devices in the next version in order to obtain high-quality, reproducible data. The most pressing need is for a new optical setup; the laser spot on the PSD from the current laser source is not localized well, limiting the quality of the strain measurements and requiring lots of tedious recalibration. Upgrading the laser source and adding a commercial lock-in would provide higher resolution and reproducibility in strain measurements. The beamsplitter and quartz tube are also not firmly attached to the foundation and must be manually readjusted every time a new device is put into the system. The new version should improve control over those two degrees of freedom by bolting everything to the foundation and adding an adjustable mirror to replace the movement previously made by the beamsplitter and tube. We have also observed some thermal drift in the gap width when the piezoactuator is engaged which is caused by thermal expansion of the pusher and which could be fixed by getting a piezoactuator with a higher temperature tolerance that is made out of Invar or a similar material.

The primary issue with the devices themselves is that the epoxy used to hold down the ends of the wires appears to instead be sliding over the wire when tensile strain is applied, preventing accurate, reproducible measurement of the tensile stress region in intrinsic VO_2. We are ac-

tively searching for another adhesive or procedure that will actually bond the wires to the substrate rather than simply set around them. Alternatives considered so far include different epoxies, spin-coated TEOS (a material that breaks down to SiO_2 when heated) or SU-8 photoresist, focused ion beam deposition of platinum contacts, and a complicated procedure involving multiple lithography and transfer steps.

In the future, we would like to measure electrical transport in nanowires that we know are under zero strain as a test of the strain setup and whatever adhesive we use. Since graphene is conductive and preliminary observations suggest VO_2 and graphene slide across each other easily without much friction, we can try to transfer a wire onto two graphene electrical contacts and etch away the substrate underneath so that the wire is suspended on the two contacts and is free to maintain its natural length at all times.

We can also use the setup to measure the effects of strain on other nanostructures which are of a similar size to the VO_2 nanowires and which can be suspended across one of our paddle chips. Examples include graphene, MoS_2, and $MoSe_2$ monolayers. Combining this with Raman spectroscopy, electrical transport and optical measurements in collaboration with Xiaodong Xu's lab should provide unprecedented insight into the mechanical properties of MoS_2 and $MoSe_2$.

VI. CONCLUSION

Despite the discovery of the metal-insulator transition more than 50 years ago, the phase diagram of VO_2 is still poorly understood, especially the M1-M2 transition. We have used a new system that can simultaneously strain and heat a VO_2 nanowire to perform direct measurements of the phase diagram of an Al-doped VO_2 wire and are the first (to the best of our knowledge) group to observe, measure, and control an M1-M2 interphase boundary in VO_2. Our setup, while still in need of improvement, could provide new insights into (among other things) why M1 and M2 have similar electrical and optical properties despite differences in their crystal structure, as well as precisely mapping the location of the two metal-insulator boundaries in VO_2 across a wide range of strain and temperature.

Acknowledgments

Thanks to my advisor David Cobden, Jae Park, and everyone else in the Nanodevice Physics Lab for helping to make my summer productive and enjoyable. Thanks to Deep Gupta, Alejandro Garcia, Janine Nemerever, and Linda Vilett for organizing the UW physics REU, and to the National Science Foundation for funding it.

* Electronic address: binghame@unc.edu; URL: http://www.elibingham.com/

[1] Imada, M., Fujimori, A., Tokura, Y., "Metal-Insulator Transitions", Rev. Mod. Phys. **70**, 1039–1263 (1998).

[2] Wei, J., Wang, Z., Chen, W., Cobden, D., "New aspects of the metal-insulator transition in single-domain vanadium oxide nanobeams", Nature Nanotechnology **4**, 420-424 (2009).

[3] Schneider, G., Calado, V., Zandbergen, H., Vandersypen, L., Dekker, C., "Wedging Transfer of Nanostructures", Nano Lett., **10** (5), 1912–1916 (2010).

[4] Thomas Moldt, Axel Eckmann, Philipp Klar, Sergey V. Morozov, Alexander A. Zhukov, Kostya S. Novoselov, and Cinzia Casiraghi, "High-Yield Production and Transfer of Graphene Flakes Obtained by Anodic Bonding", ACS Nano **5 (10)**, 7700-7706 (2011).

[5] Cavalleri, A., Tóth, Cs., Siders, C.W., Squier, J.A., "Femtosecond Structural Dynamics in VO2 during an Ultrafast Solid-Solid Phase Transition", Phys. Rev. Lett. **87** (237401) (2001).

[6] Lu, S., Hou, L., Gan, F., "Surface analysis and phase transition of gel-derived VO2 thin films", Thin Solid Films **353** (1), (1999)